Sodium and potassium monolayers on Be(0001) investigated by photoemission and electronic structure calculations

J. Algdal,[1] T. Balasubramanian,[2] M. Breitholtz,[1] V. Chis,[3] B. Hellsing,[3] S.-Å. Lindgren,[1] and L. Walldén[1]
[1]*Applied Physics Department, Chalmers University of Technology, SE-412 96 Göteborg, Sweden*
[2]*MAX Laboratory, Lund University, SE-221 00 Lund, Sweden*
[3]*Physics Department, Göteborg University, SE-412 96 Göteborg, Sweden*
(Received 17 March 2008; published 5 August 2008)

Photoemission spectra show that Be(0001) surface states shift to lower energy with increasing Na or K coverage in the monolayer range. At an intermediate monolayer coverage a quantum well state appears near the Fermi edge and shifts to lower energy reaching saturation energy at full monolayer coverage. At full monolayer coverage low energy electron diffraction shows 2×2 order for K while Na forms an incommensurate close-packed structure aligned with the substrate. As a result of the different structures, the photoemission spectra show qualitative differences that are explained by diffraction. *First-principles* calculations for Be(0001) and $p(2\times2)$K/Be(0001) reproduce reasonably the measured energy shifts and dispersions. Spectra recorded for the shallow alkali-metal core levels show that the adlayer is inhomogeneous in an intermediate coverage range. While this is not noted when the valence state energies are measured a linewidth change observed for one of the surface states is ascribed to this inhomogeneity. It is suggested that the onset of inhomogeneity is associated with the occupation of states in the quantum well band. Occupation of these states, which are highly localized to the adlayer, gives metal character to the layer over an increasing area as the coverage is increased making the film homogeneous at high monolayer coverage. An anomalous emission line is observed for both Na and K as a low energy companion to the quantum well state line becoming increasingly separated from this as the coverage increases. We suggest that the satellite is due to an energy loss associated with collective oscillations in the overlayer.

DOI: 10.1103/PhysRevB.78.085102 PACS number(s): 79.60.Dp, 73.20.At, 73.21.−b, 71.15.Mb

I. INTRODUCTION

We have used angle-resolved photoemission to study the Na/Be(0001) and K/Be(0001) systems in mainly the monolayer coverage range and also observed low energy electron diffraction (LEED) patterns at full monolayer coverage. After noting that a full monolayer of K has 2×2 order, a first-principles calculation of atomic and electronic structure was made for this system.

Be(0001) has been extensively studied by photoemission. Aside from providing information about bulk and surface states with respect to dispersion, symmetry, and charge distribution,[1–5] the extreme properties of Be, high vibration frequencies, and a strong electron-phonon coupling for surface-state electrons, the results have been important for advancing the understanding of how phonons affect photoemission line shapes and linewidths for valence as well as core electrons.[6–11] Another unusual property of Be(0001) of interest when a metal layer is adsorbed is the distinct difference between the bulk and surface electronic structure semimetal in the bulk and metal near the surface.

Characteristic of Be(0001) is the existence of a band gap, which is wide with respect to energy and lateral wave vector. The gap provides confinement over the entire energy-wave-vector range of occupied electronic states in an adsorbed alkali-metal film. Due to the confinement all state characteristics of the overlayer systems are expected to be discrete as for a thin film in vacuum with the difference that the tail on the substrate side of the adsorbed film is oscillatory. The boundary conditions are thus favorable for realizing simple metal quantum wells with all states confined and discrete. Only few substrates meet this requirement considering also that the sample must be conducting for photoemission to be applicable. Graphite is an alternative but when an alkali metal is adsorbed, a low temperature is needed to avoid intercalation or, for Na, three-dimensional (3D) growth.[12–14]

A motivation for finding systems that realize near ideal metal quantum wells is that these provide unique opportunities to study many aspects of solid-state properties as witnessed by the wide range of experiments performed on the metal quantum well systems already uncovered.[15–22] In the present work the emphasis is on the characterization of Na/Be(0001) and K/Be(0001) in the monolayer range but some measurements made at higher coverage indicate that both systems are benign in the sense that additional layers can be grown with atomic layer defined thickness.

In part the results are as expected and foreshadowed by those reported for the Li/Be(0001) system.[23,24] Surface states shift gradually with increasing monolayer coverage and the same holds for a quantum well state (QWS), which becomes populated above an intermediate coverage. The gradual energy shifts could suggest that the adlayer is homogeneous with uniform adatom density and electronic structure. However, the spectra obtained for the shallow alkali-metal core levels reveal an inhomogeneity in an intermediate coverage range in which the overlayer obtains metal character. Furthermore the combination of photoemission and inverse photoemission data obtained for Li indicated that the population of the QWS does not occur via a gradual downshift of the energy across the Fermi level in the manner observed for Na or Cs covered Cu(111).[25–27] Instead the QWS appears separated from the Fermi edge at all coverages for which it was observed.

At full monolayer coverage the photoemission spectra of K/Be(0001) and Na/Be(0001) show qualitative differences although the electronic structures are quite similar. As discussed below these differences may be ascribed to diffraction, the 2×2 ordered K layer producing emission lines not noted for the close-packed but incommensurate Na layer.

Perhaps most interesting among the observations is an emission line noted for both Na and K and previously for Li.[23] The line appears in concert with the quantum well state line becoming increasingly separated from this as the alkali-metal coverage is increased. The energy-band calculation predicts no state that may account for the line and as far as we can understand there are no single-particle excitations that could explain the line in terms of an energy loss. We suggest that the line is due to an energy loss associated with a collective oscillation involving the quantum well state electrons.

II. EXPERIMENT

The angle-resolved photoemission spectra are recorded in the MAX synchrotron radiation laboratory at BL33, which covers the photon energy range of 15–150 eV. The Be(0001) surface was prepared by cycles of Ar-ion sputtering followed by heating repeated in cycles until the zone-center surface state appeared as distinct as in a recent report.[9] The alkali metal was evaporated from heated glass ampoules broken *in situ* and held at constant temperature during an experimental run. For deposition and measurement the sample holder had to be moved between manipulators in the spectrometer and preparation chambers. In the spectrometer chamber and in the chamber used for K deposition, the sample holder was in contact with a LN_2 filled tube that gives a sample temperature of around 100 K

Spectra recorded before and after the sample had been exposed to the LEED beam for a few minutes showed that this degraded the sample with respect to measured peak intensities. Apart from this contamination effects seem modest. After leaving a sample with a full alkali-metal monolayer in vacuum for 12 h without cooling contamination gives an increased intensity at around 8 eV binding energy. This is typical of oxygen which is the main contaminant in Be. In spite of this the emission lines of present interest are still observed with reduced intensity but with little change in the binding energy.

III. CALCULATIONS

The electronic structure calculations were performed with the total energy, plane-wave code PWSCF,[28] which is based on the density-functional theory (DFT). We adopt norm-conserving pseudopotentials for K and Be and the local-density approximation for the exchange and correlation energy. A kinetic cutoff of 300 eV was used for the plane-wave basis and the finite temperature smearing of first-order Methfessel-Paxton type[29] was set to 0.68 eV.

The atomic arrangement of (2×2)K/Be(0001) was obtained by minimizing the total energy with respect to the positions of the K and Be atoms using a 17 atomic layer thick Be slab as substrate. The supercell contains four Be atoms in each layer and one K atom on the vacuum sides of the cell. In order to marginalize surface to surface interaction through the vacuum region, the surfaces were separated by 22.5 (Be) and 26.5 Å (K/Be) of vacuum.

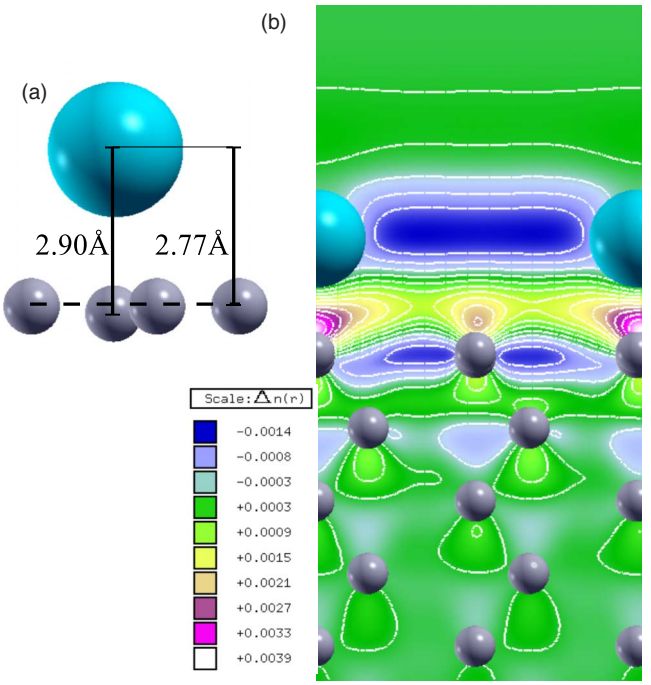

FIG. 1. (Color online) (a) Optimized structure of a K (2×2) monolayer on Be(0001). (b) Calculated electron-density redistribution in the $(11\bar{2}0)$ plane due to adsorption of a K (2×2) monolayer onto Be(0001).

The Be(0001) slab was relaxed until the resulting force acting on an atom was less than 25 meV/Å. Our calculation gives an expansion of the first and second interlayer distances by 3.2% and 0.93%, respectively, while the relaxation of deeper layers is negligible. A sizable first interlayer expansion is in agreement with previous calculations, 3.8%,[30] and LEED results, 5.8%.[31] As for the first interlayer distance our second interlayer separation is somewhat smaller than found in the previous calculation, 2.2%.[30]

Based on the optimized structure for the Be(0001) slab three different K adsorption sites were investigated. The on top and the two different hollow sites were compared with respect to total energy after having fully relaxed all atoms in a two step procedure. In the first step the adsorbed K atom was allowed to relax freely but the structure optimized for the Be substrate was kept rigid. This resulted in the following order of preference: (1) fcc hollow, (2) hcp hollow, and (3) on top, with 12 meV lower energy for the fcc site. In the second step all atoms are allowed to relax. The result is that the on-top site is favored by 15 meV/K atom. With the atom in this site there is, in the second step, an inward relaxation for both the K atom and the uppermost Be layer such that the K-Be distance is reduced by 2.6%. Furthermore, as shown in Fig. 1, the adatom induces a rumpling of the Be surface layer. The on-top K atom resides 2.9 Å above the Be atom and this distance is 0.13 Å larger than the distance to the

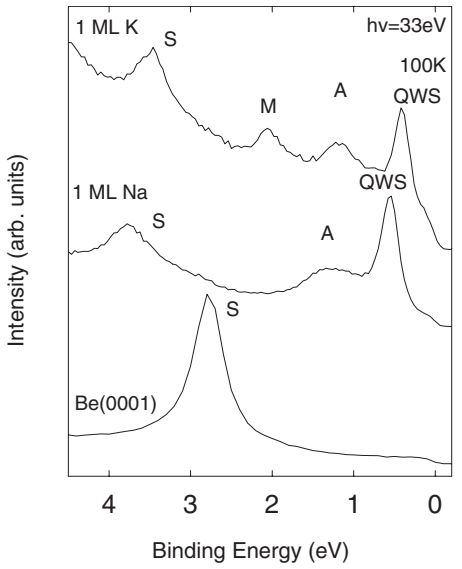

FIG. 2. Photoemission spectra recorded at 33 eV photon energy along the surface normal for Be(0001) (lower spectrum) and this substrate covered with 1 ML of Na or 1 ML of K. The adsorbates shift the $\bar{\Gamma}$ surface state (labeled S in the diagram) to higher binding-energy and quantum well states (QWS in the diagram) are observed at around 0.5 eV binding energy. The peak labeled M, observed for K but not for Na, is explained by the different structures of the two overlayers. Similar peaks, labeled A, are observed for both Na and K and these are not well understood. The light is incident at angle of 45° and polarized in the incidence plane.

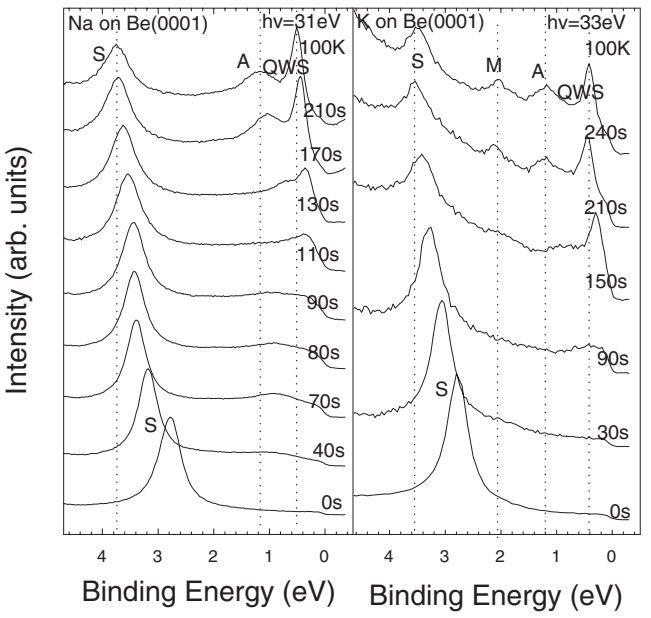

FIG. 3. Photoemission spectra recorded along the surface normal of Be(0001) for different Na (left panel) and K coverages (right panel). The coverages are given via the evaporation times in seconds. Full monolayer coverages are obtained after around 210 s for Na and 240 s for K. For labeling and explanation of peaks we refer to Fig. 2 and to the text.

plane of the surrounding Be atoms in the top layer.

The adsorption of a K monolayer gives a work-function change and a redistribution of the charge compared to that of the constituents. The calculated work function of Be(0001) is 4.9 eV and is reduced by 2.6 eV when the K layer has been adsorbed. The charge-density redistribution shown in Fig. 1 was obtained by summation of the charge-density distributions of a freestanding K monolayer and the Be(0001) slab and subtraction of the sum from the charge-density distribution for the overlayer system. One notes that most of the charge accumulation is found in the interface region. This increase is mainly due to transfer from the K layer but there is also a small contribution from the first and second Be layers.

The energy-band structure was calculated along high-symmetry directions of the respective Brillouin zones of Be(0001) and (2×2)K/Be(0001). The bands and the wave functions for the states of interest will be presented below in connection to the experimental results.

IV. RESULTS

A. Band structure and diffraction effects

The differences and similarities between the photoemission spectra of the two systems are illustrated in Fig. 2, which shows energy distributions recorded along the surface normal for Be(0001) and this substrate covered with a full monolayer of Na or K. Like most of the spectra recorded in the present work the results in Fig. 2 were obtained at photon energies in the 30–35 eV range since all the states of interest then appear with reasonable intensity. The spectrum recorded for the clean substrate is dominated by the surface-state peak at 2.8 eV binding energy. As alkali metal is deposited this state shifts to lower energy gradually with increasing surface coverage approaching a saturation binding energies of 3.7 eV for Na and 3.4 eV for K (Fig. 3). The peaks labeled QWS in Fig. 2 are due to quantum well like states in the adsorbed monolayer. A corresponding state was observed for 1 monolayer (ML) of Li.[23] The QWS lines appear near the Fermi edge at a certain coverage and shift to higher binding energy with saturation at 0.55 and 0.40 eV binding energies for Na and K, respectively (Fig. 3). Peak A is poorly understood and will be discussed last in this section. The shown spectra were recorded for a cooled sample. Spectra recorded with the sample at RT show the same features although somewhat less distinct. At the lower temperature the QWS binding energies at saturation are slightly higher by around 0.15 eV for Na and 0.1 eV for K. A possible reason is that more atoms may be accommodated in the monolayer at the lower temperature.

Using saturation of the binding energy shifts as demarcation of full monolayer coverage the LEED patterns were recorded at this stage (Fig. 4). These show that K atoms form a 2×2 overlayer as might be expected from the relative sizes of K and Be atoms. The Na atoms are smaller and form a close-packed incommensurate overlayer with a surface mesh corresponding to 1.65×1.65 and with the symmetry directions along those of the substrate although with a small azimuthal elongation of the spots.

The peak labeled M in Fig. 2 appears only for potassium and becomes prominent only at high monolayer coverage.

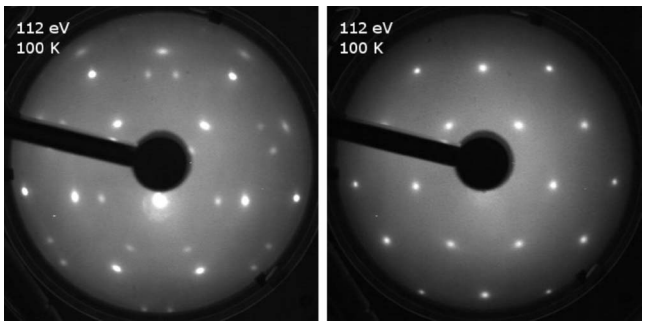

FIG. 4. LEED patterns obtained at full monolayer alkali-metal coverage on Be(0001). For Na (left panel), the overlayer forms an incommensurate structure, surface mesh approximately 1.65×1.65, aligned with the substrate although with some azimuthal disorder. For K the pattern corresponds to 2×2 order (right panel). Both patterns are recorded at 100 K with an electron energy of 112 eV. The appearance of the zero-order spot just below the center shadow in the left-hand panel is explained by a somewhat larger incidence angle in that case.

The origin of this peak becomes evident from the LEED pattern and the emission angle dependence of the photoemission spectra (Fig. 5). Figure 6 shows the dispersion of states along the $\bar{\Gamma}$-$\bar{M}$ direction obtained from the angle dependence of the spectra shown in Fig. 5. For comparison the calculated bands for slabs of Be(0001) and $p(2\times2)$K/Be(0001) are shown in Fig. 7. For Be(0001) the calculation shows the surface states at $\bar{\Gamma}$ and $\bar{M}$ with binding energies (2.7 and 1.8 eV, respectively) near the experimental values (2.8 and 1.8 eV). The main qualitative difference between the two calculated band structures is that a QWS band appears for the overlayer case extending 0.56 eV below the Fermi energy at $\bar{\Gamma}$. Aside from this there is an increased number of bands for

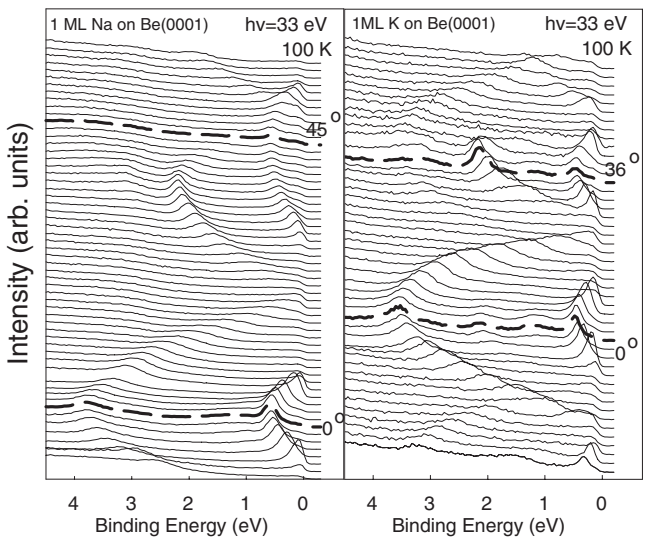

FIG. 5. Photoemission spectra recorded with 33 eV photon energy at different polar angles probing downshifted Be surface states and quantum well states along $\bar{\Gamma}$-$\bar{M}$ for Na (left panel) and K (right panel) at 1 ML coverage. The *p*-polarized light beam is in the plane of measurement and incident at angle of 45°.

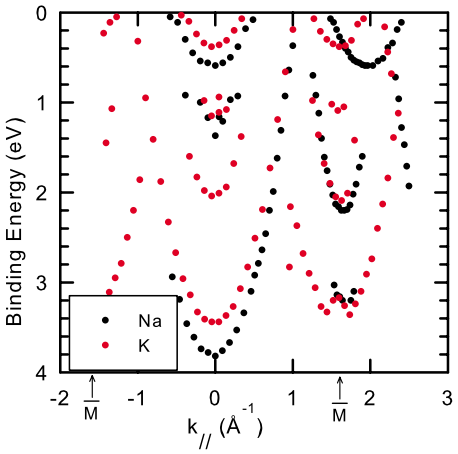

FIG. 6. (Color online) Binding energies, read off from the spectra in Fig. 5, plotted versus parallel wave vector for 1 ML of Na (black dots) and 1 ML of K (red dots). The arrows at ±1.59 Å^{-1} on the horizontal axes indicate opposite $\bar{M}$ points of the Be (0001) surface Brillouin zone.

the $p(2\times2)$K/Be(0001) structure due to the folding of bands into the smaller Brillouin zone defined by the overlayer. In this zone the surface state at the $\bar{M}$ point of the larger Be(0001) zone is found at $\bar{\Gamma}$.

From the dispersion it is clear that peak M in Fig. 2 is due to the upper surface state at the $\bar{M}$ point of the surface Brillouin of the substrate. Upon adsorption the state has become downshifted by 0.4 eV for Na and by 0.3 eV for K from the energy for clean Be(0001). The shift calculated for K is 0.2 eV. Also the larger shift of the $\bar{\Gamma}$ surface state, 0.7 eV for K, is well reproduced by the calculation (0.70 eV). Although the shift of the $\bar{\Gamma}$ state is large there is only a modest increase in the number of electrons in the band since the dispersion is changed. The experiment (calculation) gives effective band masses m^*/m of 1.25 (1.25) for Be(0001) and 1.14 (1.15)

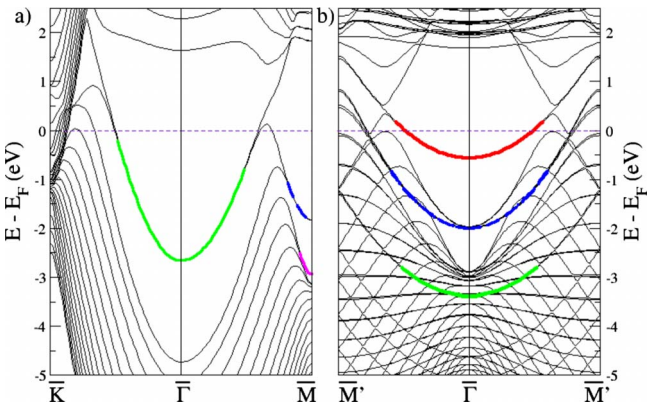

FIG. 7. (Color online) Calculated band structure (a) for 17 atomic layer Be(0001) and (b) for this film covered with 2×2 ordered K atoms occupying on top sites. For clean Be(0001) there are surface bands with binding energies of 2.7 eV at $\bar{\Gamma}$ and 1.8 and 2.9 eV at $\bar{M}$. For the adsorbate covered substrate the corresponding energies are 3.4, 2.0, and 2.9 eV, respectively. In addition there is a quantum well state band extending 0.56 eV below E_F.

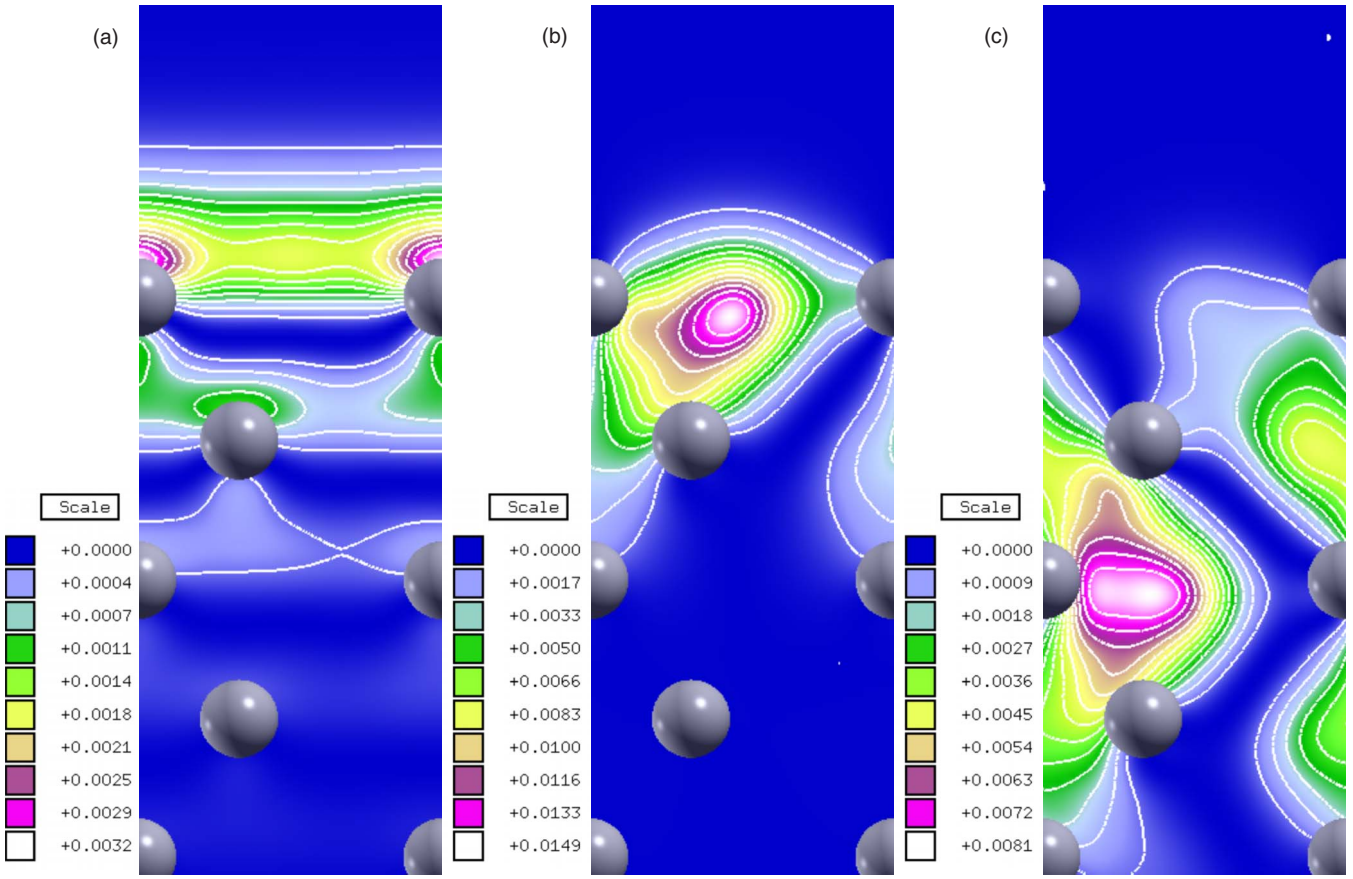

FIG. 8. (Color online) Calculated electron density for Be(0001) in (a) the $(11\bar{2}0)$ plane for the $\bar{\Gamma}$ surface state, (b) the upper $\bar{M}$ surface state, and (c) the lower $\bar{M}$ surface state.

when the substrate is covered with 1 ML K. Assuming the length of Fermi wave vector in the $\bar{\Gamma}$-$\bar{M}$ direction to be representative, the population of the $\bar{\Gamma}$ surface band increases by around 5% from 0.7 electrons per Be atom for the clean substrate. A more significant change for the charge balance at the interface is that the state has shifted to energies closer to the lower edge of the bulk band gap at around 4.8 eV (4.3 eV) below E_F according to experiment (calculation).[2] More of the charge is therefore deposited further inside the substrate [Figs. 8(a) and 9(a)]. In addition the tail outside the substrate becomes longer than for the clean surface due to the attractive potential in the overlayer. Also the upper $\bar{M}$ state shifts toward the edge of the bulk gap but in this case, at least in the $(11\bar{2}0)$ plane, the charge is redistributed mainly in the lateral direction [Figs. 8(b) and 9(b)].

For the QWS bands the dispersion is repeated with a lateral period that agrees well with the LEED patterns. In the case of Na one might expect the substrate to introduce another repetition period for the QWS band but this is not observed. Regarding periodicity it is as if there had been no substrate. The dispersion of the QWS bands corresponds to band masses m^*/m of 1.65 for Na and 1.55 for K and according to the band calculation it is 1.05 for K. As noted in Table I where experimental and calculated energies and effective masses may be compared, the only significant difference concerns the mass of the QWS band. The discrepancy may reflect the poor energy resolution in the calculations close to the Fermi level. This is probably due to the introduced smearing of the Fermi level to improve convergence. In these calculations the smearing parameter is 0.68 eV, which even exceeds the binding energy of 0.56 eV of the QWS at $\bar{\Gamma}$. This underestimate of the effective mass is also obtained in a previous DFT calculation for the QWS band of the saturated Na ML on Cu(111),[32] when applying a smearing parameter of 0.1 eV, which similarly slightly exceeded the binding energy at $\bar{\Gamma}$ of 0.06 eV. The measured dispersion gives occupancies of 0.54 and 0.50 electrons per alkali-metal atom for Na and K, respectively. For K also the downshifted Γ surface band appears displaced by a reciprocal-lattice vector defined by the 2×2 overlayer, while no corresponding observation is made for Na (Fig. 6).

In addition to the states discussed above Be(0001) has a second surface state or resonance at the lower edge of the bulk band gap at the $\bar{M}$ point. The state is observed only in a small range of lateral wave vectors near the $\bar{M}$ point. For the K covered surface this surface state is difficult to resolve from the downshifted and $k_{\|}$-shifted $\bar{\Gamma}$ surface state but overlap between these emission lines may give the distorted looking dispersion near the band minimum in Fig. 6. As noted in a previous calculation[33] the lower $\bar{M}$ state deposits its charge below the surface [Fig. 8(c)] and is therefore not much affected by an adsorbate.

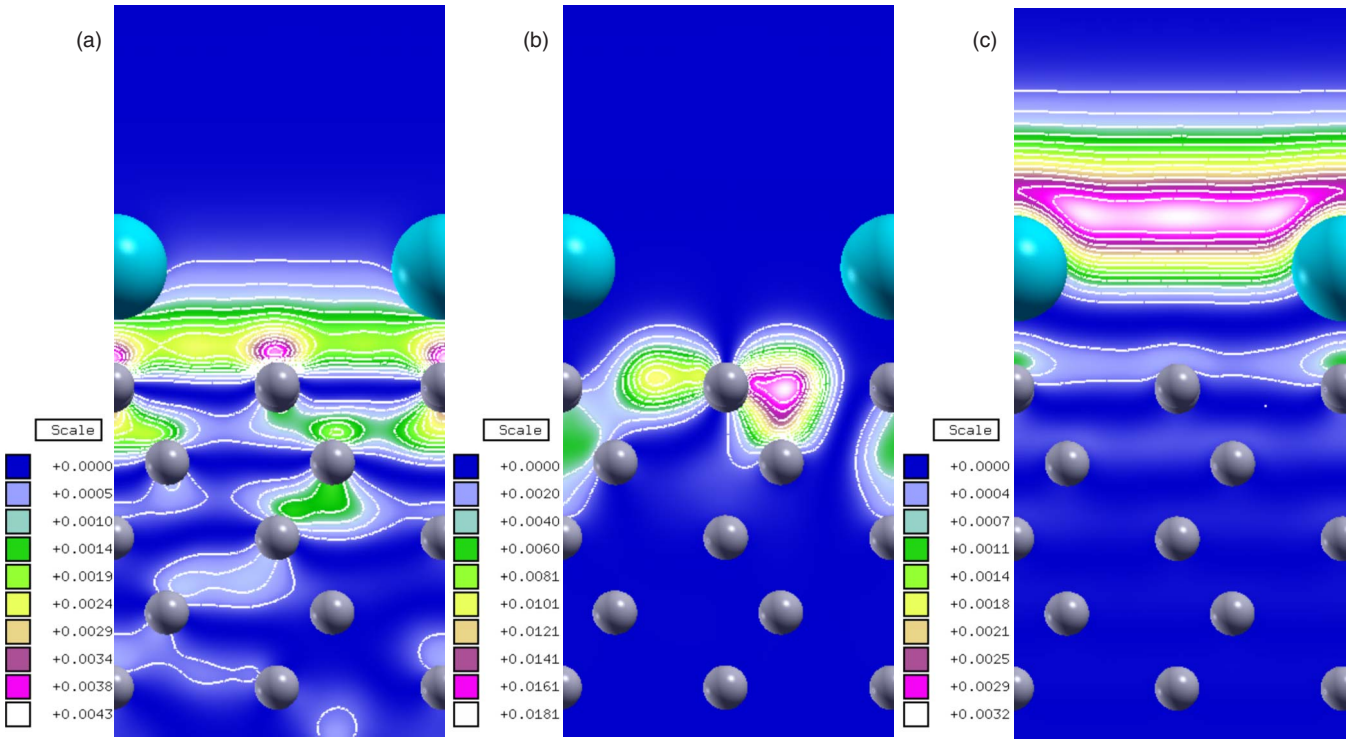

FIG. 9. (Color online) Calculated electron density at $\bar{\Gamma}$ for a K 2×2 monolayer on Be(0001)in the $(11\bar{2}0)$ plane of the substrate for (a) the downshifted Be (0001) $\bar{\Gamma}$ surface state, (b) the downshifted upper $\bar{M}$ state, (c) and the quantum well state.

Regarding peak A in Fig. 2, a similar feature was observed for Li covered Be(0001).[23] It was mentioned that it might be a loss component to the QWS line but it was believed to be due to a state translated to $\bar{\Gamma}$ by a reciprocal-lattice vector for the Li overlayer. Support for this came from the observation of a band maximum with the same energy as the peak of a reciprocal-lattice vector away from $\bar{\Gamma}$. For Na or K there is no similar coincidence with respect to energy making the interpretation in terms of umklapp unlikely. Although we will not be able to give an interpretation we report some observations. As shown in Fig. 3 peak A appears in concert with the QWS line and becomes increasingly separated from this line as the coverage increases. As for Li the peak is observed only at angles near the surface normal (Fig. 6) but for K it is observed also near $\bar{\Gamma}$ of the second zone of the overlayer. If the photon energy is changed the intensity of peak A varies approximately as the QWS peak (Fig. 10). As noted previously[34,35] the cross section for a QWS can vary rapidly with photon energy (Fig. 10). If the coverage is increased beyond the monolayer range, peak A decays in intensity. For multilayers no peak similar to A is observed in the energy range between the QWS lines and the line due to the downshifted $\bar{\Gamma}$ surface state (Fig. 11). The latter appears at approximately the same energy as for the monolayer but with reduced intensity. Only a marginal energy shift is expected since the state already at 1 ML coverage extends only with a tail in the overlayer. No satellite with an intensity comparable to peak A is observed adjacent to the $\bar{\Gamma}$ surface-state line. Although this line is broader than the QWS line one would still expect to resolve such a satellite.

TABLE I. Experimental and calculated surface and quantum well state binding energies and effective band masses for Be(0001) and alkali-metal covered Be(0001) at 1 ML coverage. Li/Be(0001) from Watson *et al.* (Ref. 23).

	$\bar{\Gamma}$				$\bar{M}_{\text{upper}}$		QWS			
	E_B (eV)		m^*/m		E_B (eV)		E_B (eV)		m^*/m	
	Expt.	Calc.	Expt.	Calc.	Expt.	Calc.	Expt.	Calc.	Expt.	Calc.
Be	2.8	2.7	1.25	1.25	1.8	1.8				
Li/Be	4.0		1.03		2.3		0.47		1.8	
Na/Be	3.7		1.19		2.2		0.55		1.65	
K/Be	3.5	3.4	1.14	1.15	2.1	2.0	0.4	0.56	1.55	1.05

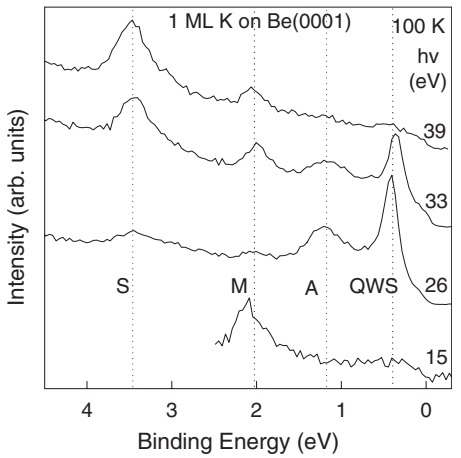

FIG. 10. Photoelectron energy spectra recorded at different photon energies along the surface normal for 1 ML K on Be(0001) showing a strong photon energy dependence for cross sections of the downshifted Be surface states, S and M, and the QWS. Note that the intensity of peak A varies in concert with the QWS intensity.

The QWS energies for multilayers (Fig. 12) change with overlayer thickness in the manner observed for many metal overlayer systems as may be explained in terms of simple model potentials.[36] At the photon energy and detection angle used to record the spectra in Fig. 10, only QWS with low binding energy gives a high intensity.

B. Shallow core levels

The gradual energy shifts observed for the valence states might suggest that the overlayer is homogeneous with respect to adatom density and electronic structure. The shallow core-level spectra shown in Fig. 12 for Na/Be(0001) demonstrate that this is not the case, at least not in a range of intermediate monolayer coverages where two emission lines

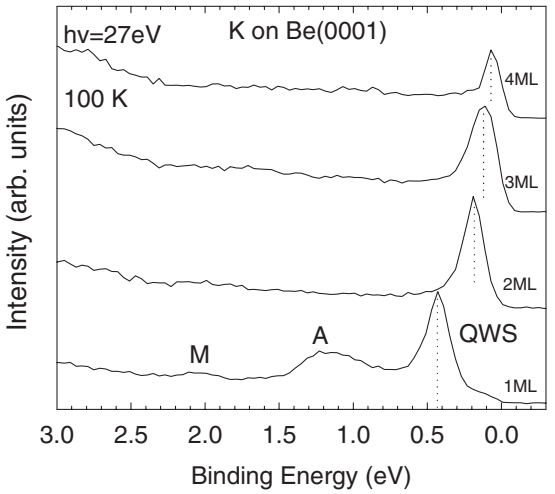

FIG. 11. Quantum well state emission lines for 1–4 ML of K on Be(0001) recorded along the surface normal at 27 eV photon energy. For overlayers thicker than 1 ML no peaks similar to A are observed.

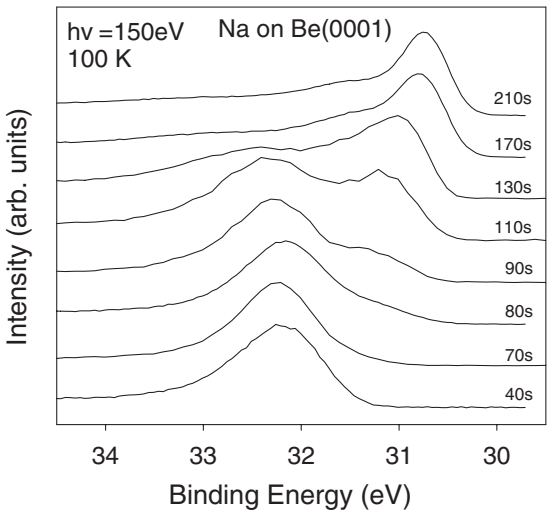

FIG. 12. Na 2*p* core-level spectra recorded at 150 eV photon energy for Na/Be(0001) at different coverages given by the deposition times. Full monolayer coverage is obtained after 210 s deposition time.

are observed. To save recording time these spectra were obtained with less resolution than required to resolve the Na 2*p* spin-orbit doublet. The line characteristic of low coverage remains at nearly constant binding energy and out of this grows a second line, which shifts to lower binding energy with increasing coverage and dominates the spectrum at high coverage. At high coverage this line is accompanied by a satellite on the low kinetic-energy side. The peak separation is around 0.7 eV at full monolayer coverage. This separation is thus similar to that between the QWS line and the anomalous peak A. While a second atomic layer might start to form before the first layer is complete, this does not explain the satellite. As shown in Fig. 13 the satellite observed for 1 ML Na falls outside the energy range of the layer dependent binding energies of thicker films. In the case of K there are bigger differences between the 3*p* binding energies for overlayers with different thicknesses (Fig. 14). Also for K a weak low energy component is noted for 1 ML but this falls at approximately the same binding energy as the K 3*p* line assigned to the uppermost atomic layer of a two atomic layer thick overlayer.

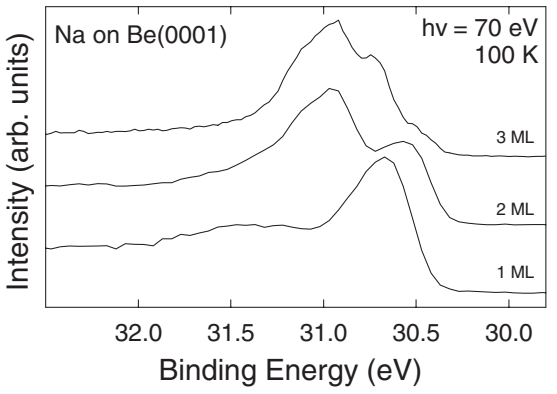

FIG. 13. Na 2*p* core-level spectra recorded at 70 eV photon energy for Be(0001) covered with 1–3 ML Na showing atomic layer dependent binding energies.

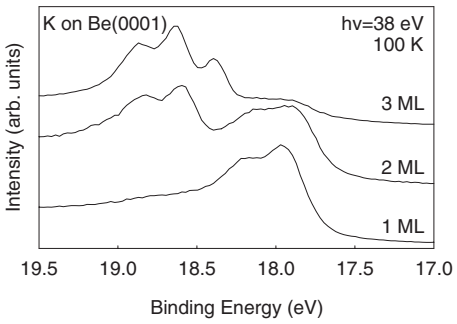

FIG. 14. K 3*p* core-level spectra recorded at 38 eV photon energy for Be(0001) covered with 1–3 ML K showing atomic layer dependent binding energies with the spin-orbit splitting resolved.

C. Coverage dependent linewidth for the $\bar{\Gamma}$ surface state

After noting in several experimental runs that the linewidth of the $\bar{\Gamma}$ surface state increases markedly in an intermediate coverage range, this was studied in detail for Na together with the Na 2*p* spectrum described above. This increase is observed at approximately the same coverage for which the QWS starts to appear. When energy shifts were monitored the coverage was typically increased in doses. Due to the time required it was suspected that the spectra recorded at high coverages might get an increased linewidth due to contamination. In the linewidth measurement the sample was therefore cleaned between each dose such that each spectrum could be recorded within minutes after the deposition. Initially upon Na deposition the width increases modestly. In an intermediate coverage range it increases more rapidly by around 100 meV reaching an almost constant value at high monolayer coverage. The coverage dependence of the linewidth is shown in Fig. 15 together with the binding energies for the states of interest.

V. DISCUSSION

A. Charge distributions, diffraction effects, and energy shifts

The states characteristic of an overlayer system are hybrids with distinctly different characters in the overlayer and the substrate. The electrons experience a potential with different spatial variations in the substrate and the adsorbed layer. The mere existence of the QWS derives from the potential variations in the direction normal to the surface and laterally there are different periods in the substrate and the overlayer. That there are two lateral periods is not expected to be important for the states observed here since each state is well anchored in either the substrate or the overlayer. As shown for K in Fig. 9(c) the QWS at $\bar{\Gamma}$ has one node in the K layer near the overlayer-substrate interface and deposits almost the entire charge in the overlayer, with maximum density outside a plane through the cores of the K atoms. This degree of confinement is extreme compared to similar cases. For alkali metals on Cu(111) the charge of the corresponding QWS, with one node in the film, is shared more equally between the substrate and the overlayer.[26,37]

In contrast to the QWS the downshifted $\bar{\Gamma}$ surface state has nearly all its charge within the substrate [Fig. 9(a)]. The energy is lower than the valence-band bottom of K metal and the state therefore extends with a tail outside the substrate although the tail is longer than for the clean Be(0001) surface. The bottom state in a square potential well is nodeless in the well and the downshifted surface state is the corresponding state for a K monolayer on Be(0001). For K the energy bands of the downshifted $\bar{\Gamma}$ and upper $\bar{M}$ states appear translated by a reciprocal-lattice vector of the overlayer (Fig. 6). This is explained by diffraction by the (2×2)K layer of the photoelectrons excited in the substrate or at the interface. No similar observation was made for Na. In that case the reciprocal-lattice vector is larger. The $\bar{M}$ states are translated to different *k* points in the overlayer zone making the diffracted intensity weaker than for the K layer when all the $\bar{M}$ states are backfolded to the $\bar{\Gamma}$ point. A possible reason for the difference between Na and K is that the heavier alkali-metal-atom scatters low energy electrons more strongly. It should also be pointed out that we did not investigate the photon energy dependence of the diffracted intensity. As in LEED the diffracted intensity will vary with electron energy with different energy dependences for different adsorbates.

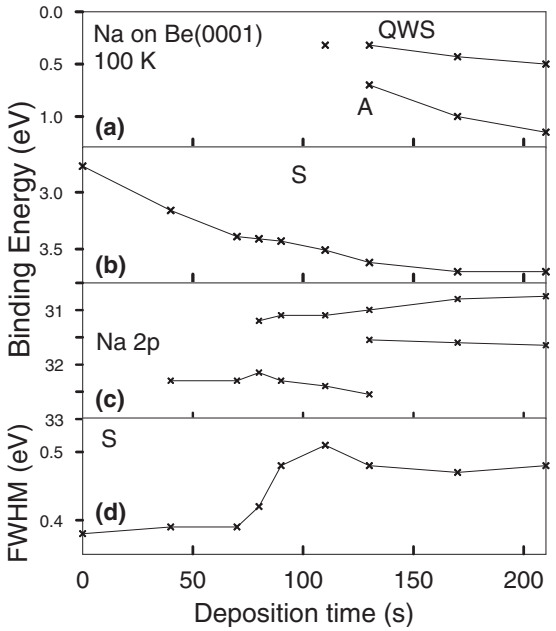

FIG. 15. Na coverage dependence for the binding energies (a) of the quantum well state and peak A, (b) of the $\bar{\Gamma}$ surface state S, (c) the Na 2*p* electrons, and (d) the width [full width at half maximum (FWHM)] of the $\bar{\Gamma}$ surface-state emission line. Full monolayer coverage is obtained after 210 s evaporation time.

B. *Linewidth of the* $\bar{\Gamma}$ surface state

The $\bar{\Gamma}$ surface state has served as a test object for theoretical calculations of hole lifetimes.[9,38] From the temperature dependence of the linewidth the electron-phonon contribution to the width could be extracted.[9] When the linewidth due to the electron-phonon interaction and the experimental resolution is accounted for there is a good agreement with the

contribution to the width from electron-electron scattering. The theoretical estimate is 265 meV, most of this, 225 meV, coming from scattering within the surface-state band, with smaller contributions from bulk states, 35 meV, and from the upper $\bar{M}$ surface state, 5 meV.[9]

As noted in Fig. 15 the linewidth of the $\bar{\Gamma}$ surface state increases significantly in the coverage range where the QWS appears near the Fermi edge. A possible reason for the onset of width increase is that the population of the QWS band opens a channel of decay for the photohole in the $\bar{\Gamma}$ surface state. This is certain to contribute to the linewidth but, considering the small overlap between the QWS and the surface state [Fig. 9(a) and 9(c)], it would be surprising to find the effect to be as large as measured. We believe that a more likely reason for the increased width is the inhomogeneity of the overlayer demonstrated by the core-level spectra (Fig. 12). The surface-state energy is no local probe and the inhomogeneity affects the binding energy weakly such that the spread in binding energy is reflected by the linewidth increase.

At high monolayer coverage the overlayer is homogeneous and there is still a larger linewidth than at low coverage. We ascribe this to the difference in electronic structure between the clean substrate surface and this surface covered with 1 ML of the alkali metal. In particular one would expect the contribution to the linewidth from bulk states to increase. One reason is the larger overlap with bulk states as the surface state extends deeper into the bulk. Furthermore, as shown for K in Fig. 7(b), the downshifted surface states is found among backfolded bulk states and may couple to these states. As a result the surface state will no longer have the discrete character it has for the clean substrate. This type of resonance broadening was recently noted to be small, <10 meV half width, but still significant for QWS in 1 ML of Na or Cs on Cu(111).[20]

C. Nonmetal-metal transition

While the binding energies of the valence electron states shift gradually with coverage, this is not observed for the Na $2p$ level. Initially upon deposition one emission line is observed but this vanishes upon continued deposition and becomes replaced by a somewhat narrower line with a gradually shifting binding energy (Fig. 12). In an intermediate coverage range both emission lines are observed (80–130 s evaporation time). At high monolayer coverage the line obtains a satellite on the low kinetic-energy side.

The coverage dependence for the Na $2p$ emission is quite similar to that noted for the Li $1s$ line of the Li/Be(0001) system.[24] The Li data included observations with inverse photoemission of the coverage dependence of the energy for an empty state near above the Fermi level. A plot versus coverage of this energy and the QWS energy measured at $k_{\|}=0$ indicated that that there is a gap between the lowest energy observed for the empty state and the highest QWS energy. As for Na and K the highest QWS energy for Li is close to the Fermi level. Based on this, the Li $1s$ data and the observed LEED patterns it was suggested that there is a discontinuous nonmetal to metal transition in the overlayer at an intermediate monolayer coverage.

The same interpretation may be made for the present systems. The metal character of the full monolayer is assured by the QWS band, which at full monolayer coverage contains around 0.54 and 0.50 electrons per alkali-metal atom for Na and K, respectively. When the QWS first appears near the Fermi edge this means that the density of states at the Fermi energy obtains a value typical of a metal. At lower coverage the states in the $\bar{\Gamma}$ surface band extends across the Fermi level but little of this charge falls in the overlayer. Assuming the QWS to have a distinct energy when it appears at a certain coverage, this would give a stepwise increase in the density of states at the Fermi level at that coverage. In practice the adatom density will not be homogeneous making the QWS energy less distinct and the onset of metal character less abrupt. Such observations are made for Na or Cs covered Cu(111) where the corresponding QWS can be observed by photoemission as it shifts with increasing coverage from above to below the Fermi energy.[26,39] With the present setup the intensity was too low to monitor states above the Fermi energy. We thus do not know whether there actually exists a QWS above the Fermi level having an energy, which may be downshifted in a gradual manner into the populated range by increasing the coverage. According to the inverse photoemission and photoemission results this is not the case for Li/Be(0001) (Ref. 24) but further information on this for the present systems would be of interest.

With the above considered it seems possible to explain the present data in terms of an almost stepwise transition to metal character in patches that become larger as the coverage is increased making the transition gradual when the whole film is considered. In the first stage the QWS is only patchwise occupied. Thus, if this electron gas is spatially inhomogeneous only a fraction of the alkali-metal atoms reside in the electron gas. This would explain the existence of two different core lines in an intermediate coverage range. Beyond this range the electron gas hangs together and only one Na $2p$ emission line is observed. As with increasing coverage the QWS band shifts to lower energy the electron density in the overlayer increases and the Na $2p$ emission line shifts to lower binding energy. In concert with the occupation of the QWS, maybe driven by this, there could be some change in the order in the overlayer. The results however indicate that this change is modest with regards to the adatom density. This is demonstrated by the gradual energy shift of the surface state and by the observation that the Na $2p$ line of the high coverage phase starts out at an energy near that observed at low coverage.

Finally we note that the present systems seem to have properties intermediate between those, which may be obtained for alkali metals deposited on metal and on graphite. Although it is not typical one may for metal substrates find a gradual change in alkali-metal core-level binding energies or excitation thresholds throughout the monolayer coverage range with a higher binding energy at low coverage when the adatoms are more ionic than at high coverage when the layer is almost neutral.[40,41] This is as observed for the high coverage phase on Be(0001). On graphite by contrast there is a

distinct change in atomic order and electronic structure in the monolayer coverage range. Beyond a coverage threshold the alkali-metal atoms form a condensed phase coexisting with a dispersed phase found at low coverage.[42] For K and Rb the high coverage phase consists of monolayer thick islands with close-packed atoms in 2×2 order.[13,43] The effect of increasing the adatom coverage is just a larger island area but no significant compression of the atoms. This is reflected by coverage independent binding energies for core and valence states for the high coverage phase. As demonstrated by a LEED and core-level study of K/Ag(100), one system can show both of the two types of behavior referred to above.[44] At 90 K core-level binding energies change in a gradual manner as the coverage is increased but at 220 K this is only observed in a low coverage range. Beyond approximately 0.2 ML coverage an island phase is observed which is reflected in the spectra by a nearly stepwise change in binding energy, this remaining almost constant when the coverage is increased.

D. Anomalous peak

Peak A in Fig. 2 could be due to an energy loss with the QWS line as the primary. Since there is a similar separation in energy between the Na $2p$ components observed at high monolayer coverage (Fig. 12), the low energy component may be a loss satellite due to the same excitation. We find no single-particle excitations that could account for a loss peak and speculate that the loss is due to collective oscillations in the overlayer. For the clean Be(0001) a loss due acoustic plasmons in the surface layer was recently observed and the dispersion was explained quantitatively[45] using a model predicting this type of excitation for Be(0001).[46] The results were obtained by electron energy-loss spectroscopy and the present data suggest that similar experiments would be of interest for alkali-metal covered Be(0001). The QWS electrons form a very thin sheet of electron gas in the outer region of the monolayer and this may be expected to have an important influence on the collective oscillations near the surface. Plasmon excitations have been observed previously for adsorbed alkali-metal monolayers by electron-energy loss spectroscopy[40,47–50] but have not showed up in photoemission spectra.

VI. SUMMARY

The $\bar{\Gamma}$ surface state of Be(0001) shifts gradually to lower energy with increasing Na or K coverage in the monolayer range. At least for Na/Be(0001) which was studied in detail the gradual shift masks the inhomogeneity evident from the shallow core-level spectra in an intermediate coverage range. In this range a quantum well state characteristic of 1 ML coverage becomes occupied marking the onset of metal character locally as well as the onset of inhomogeneity. According to our interpretation the inhomogeneity is noted as a linewidth change for the $\bar{\Gamma}$ surface state. Although the population of the quantum well state opens a channel of decay for the photohole in the $\bar{\Gamma}$ surface state, we believe this to give a minor increase in the linewidth. At full monolayer coverage the spectra for K and Na show qualitative differences, which reflect the different structures obtained with prominent diffraction effects noted for the commensurate K monolayer. The band structure obtained from a structure optimized DFT calculation made for 2×2 ordered K on Be(0001) agrees well with the experiment. An unexplained emission line is observed for both 1 ML Na and K. The data indicate that this is a loss companion to the quantum well state emission peak. We suggest that some collective mode is excited involving the QWS electrons, which form a thin sheet of electron gas in the adsorbed monolayers.

ACKNOWLEDGMENTS

We gratefully acknowledge discussions with Evgueni Chulkov and Viatcheslav Silkin regarding possible collective surface excitations of the systems studied and financial support from the Swedish Research Council.

[1] U. O. Karlsson, S. A. Flodström, R. Engelhardt, W. Gadeke, and E. E. Koch, Solid State Commun. **49**, 711 (1984).
[2] E. Jensen, R. A. Bartynski, T. Gustafsson, E. W. Plummer, M. Y. Chou, M. L. Cohen, and G. B. Hoflund, Phys. Rev. B **30**, 5500 (1984).
[3] R. A. Bartynski, E. Jensen, T. Gustafsson, and E. W. Plummer, Phys. Rev. B **32**, 1921 (1985).
[4] I. Vobornik, J. Fujii, M. Mulazzi, G. Panaccione, M. Hochstrasser, and G. Rossi, Phys. Rev. B **72**, 165424 (2005).
[5] I. Vobornik, J. Fujii, M. Hochstrasser, D. Krizmancic, C. E. Viol, G. Panaccione, S. Fabris, S. Baroni, and G. Rossi, Phys. Rev. Lett. **99**, 166403 (2007).
[6] M. Hengsberger, D. Purdie, P. Segovia, M. Garnier, and Y. Baer, Phys. Rev. Lett. **83**, 592 (1999).
[7] M. Hengsberger, R. Frésard, D. Purdie, P. Segovia, and Y. Baer, Phys. Rev. B **60**, 10796 (1999).
[8] S. LaShell, E. Jensen, and T. Balasubramanian, Phys. Rev. B **61**, 2371 (2000).
[9] V. M. Silkin, T. Balasubramanian, E. V. Chulkov, A. Rubio, and P. M. Echenique, Phys. Rev. B **64**, 085334 (2001).
[10] J. N. Andersen, T. Balasubramanian, C.-O. Almbladh, L. I. Johansson, and R. Nyholm, Phys. Rev. Lett. **86**, 4398 (2001).
[11] A. Eiguren, S. de Gironcoli, E. V. Chulkov, P. M. Echenique, and E. Tosatti, Phys. Rev. Lett. **91**, 166803 (2003).
[12] M. Breitholtz, T. Kihlgren, S.-Å. Lindgren, H. Olin, E. Wahlström, and L. Walldén, Phys. Rev. B **64**, 073301 (2001).
[13] J. Algdal, M. Breitholtz, T. Kihlgren, S.-Å. Lindgren, and L. Walldén, Phys. Rev. B **73**, 165409 (2006).
[14] J. Algdal, T. Balasubramanian, M. Breitholtz, T. Kihlgren, and L. Walldén, Surf. Sci. **601**, 1167 (2007).
[15] T.-C. Chiang, Surf. Sci. Rep. **39**, 181 (2000).
[16] S.-Å. Lindgren and L. Walldén, *Handbook of Surface Science*

(Elsevier, New York, 2000), Vol. 2, p. 899.
[17] M. Milun, P. Pervan, and D. P. Woodruff, Rep. Prog. Phys. **65**, 99 (2002).
[18] J. Kröger, M. Becker, H. Jensen, Th. von Hofe, N. Néel, L. Limot, R. Berndt, S. Crampin, E. Pehlke, C. Corriol, V. M. Silkin, D. Sanchez-Portal, A. Arnau, E. V. Chulkov, and P. M. Echenique, Prog. Surf. Sci. **82**, 293 (2007).
[19] G. Hoffmann, R. Berndt, and P. Johansson, Phys. Rev. Lett. **90**, 046803 (2003).
[20] C. Corriol, V. M. Silkin, D. Sanchez-Portal, A. Arnau, E. V. Chulkov, P. M. Echenique, T. von Hofe, J. Kliewer, J. Kröger, and R. Berndt, Phys. Rev. Lett. **95**, 176802 (2005).
[21] Y.-F. Zhang, J.-F. Jia, T.-Z. Han, Z. Tang, Q.-T. Shen, Y. Guo, Z. Q. Qiu, and Q. K. Xue, Phys. Rev. Lett. **95**, 096802 (2005).
[22] M. Fuyuki, K. Watanabe, D. Ino, H. Petek, and Y. Matsumoto, Phys. Rev. B **76**, 115427 (2007).
[23] G. M. Watson, P. A. Brühwiler, E. W. Plummer, H.-J. Sagner, and K.-H. Frank, Phys. Rev. Lett. **65**, 468 (1990).
[24] G. M. Watson, P. A. Brühwiler, H. J. Sagner, K.-H. Frank, and E. W. Plummer, Phys. Rev. B **50**, 17678 (1994).
[25] A. Carlsson, B. Hellsing, S.-Å. Lindgren, and L. Walldén, Phys. Rev. B **56**, 1593 (1997).
[26] M. Breitholtz, V. Chis, B. Hellsing, S.-Å. Lindgren, and L. Walldén, Phys. Rev. B **75**, 155403 (2007).
[27] J. Kliewer and R. Berndt, Phys. Rev. B **65**, 035412 (2001).
[28] S. Baroni, A. Dal Corso, S. de Gironcoli, and P. Giannozzi (http://www.pwscf.org).
[29] M. Methfessel and A. T. Paxton, Phys. Rev. B **40**, 3616 (1989).
[30] P. J. Feibelman, Phys. Rev. B **46**, 2532 (1992).
[31] H. L. Davis, J. B. Hannon, K. B. Ray, and E. W. Plummer, Phys. Rev. Lett. **68**, 2632 (1992).
[32] J. M. Carlsson and B. Hellsing, Phys. Rev. B **61**, 13973 (2000).
[33] E. V. Chulkov, V. M. Silkin, and E. N. Shirykalov, Surf. Sci. **188**, 287 (1987).
[34] A. Carlsson, D. Claesson, S.-Å. Lindgren, and L. Walldén, Phys. Rev. B **52**, 11144 (1995).
[35] M. Milun, P. Pervan, B. Gumhalter, and D. P. Woodruff, Phys. Rev. B **59**, 5170 (1999).
[36] S.-Å. Lindgren and L. Walldén, Phys. Rev. Lett. **59**, 3003 (1987); **61**, 2894 (1988).
[37] S.-Å. Lindgren and L. Walldén, Phys. Rev. B **38**, 3060 (1988).
[38] I. Yu. Sklyadneva, E. V. Chulkov, P. M. Echenique, and A. Eiguren, Surf. Sci. **600**, 3792 (2006).
[39] A. Carlsson, S.-Å. Lindgren, C. Svensson, and L. Walldén, Phys. Rev. B **50**, 8926 (1994).
[40] S.-Å. Lindgren and L. Walldén, Phys. Rev. B **22**, 5967 (1980).
[41] J. N. Andersen, E. Lundgren, R. Nyholm, and M. Qvarford, Surf. Sci. **289**, 307 (1993).
[42] Z. Y. Li, K. M. Hock, and R. E. Palmer, Phys. Rev. Lett. **67**, 1562 (1991).
[43] N. Ferralis, K. Pussi, S. E. Finberg, J. Smerdon, M. Lindroos, R. McGrath, and R. D. Diehl, Phys. Rev. B **70**, 245407 (2004).
[44] S. Modesti, C. T. Chen, Y. Ma, G. Meigs, P. Rudolf, and F. Sette, Phys. Rev. B **42**, 5381 (1990).
[45] B. Diaconescu, K. Pohl, L. Vattuone, L. Savio, P. Hoffmann, V. Silkin, J. M. Pitarke, E. Chulkov, P. Echenique, D. Farias, and M. Rocca, Nature (London) **448**, 57 (2007).
[46] V. M. Silkin, A. García-Lekue, J. M. Pitarke, E. V. Chulkov, E. Zaremba, and P. M. Echenique, Europhys. Lett. **66**, 260 (2004).
[47] A. U. MacRae, K. Müller, J. J. Lander, J. Morrison, and J. C. Phillips, Phys. Rev. Lett. **22**, 1048 (1969).
[48] S. Thomas and T. W. Haas, Solid State Commun. **11**, 193 (1972).
[49] S. Andersson and U. Jostell, Faraday Discuss. Chem. Soc. **60**, 255 (1975).
[50] U. Jostell, Surf. Sci. **82**, 333 (1979).